Performance improvement of PEM fuel cells using air channel indentation;
Part I: Mechanisms to enrich oxygen concentration in catalyst layer

A.Ghanbarian[1,3] and M.J. Kermani[2,3,4*]

[1]Department of Aerospace Engineering, Amirkabir University of Technology (Tehran Polytechnic), Tehran, Iran
[2]Fuel Cell Laboratory, Energy Conversion Research Lab, Department of Mechanical Engineering, Amirkabir University of Technology (Tehran Polytechnic), Tehran, Iran
[3]Renewable Energy Research Center (RERC), Amirkabir University of Technology (Tehran Polytechnic), Tehran, Iran
[4]Adjunct Research Fellow, Zentrum fuer Sonnenenergie und Wasserstoff- Forschung (ZSW)-ECB, Ulm, Germany

Article Information

Keywords

Abstract

A three dimensional, compressible, steady, one phase flow of reactant-product mixture in the air side electrode of proton exchange membrane fuel cell (PEMFC) is numerically studied in this paper. The mixture is composed of three species: oxygen, nitrogen and water vapor. The performance of the cell is enhanced by partial blockage of the flow field channels. Various types of these blocks also called as dents in this study are considered. Examples of the dent profile shapes are: square (labeled as SQ case in this paper), semicircle (or SC) and trapezoid (or TR), and the enhancements are compared with that of no dent (or ND) case. It is observed that channel indentation can enhance the content of oxygen concentration at the face of catalyst layer up to 18%. It is noted that the content of oxygen at the face of catalyst is the driving moment for the kinetics of reaction within the catalyst layer. Hence channel indentation can be considered as a proper mechanism to enhance the performance of fuel cells. In this paper only the increasing of driving moment is discussed and the analysis of net power enhancement will be discussed later in another paper.

1. Introduction

Fuel cells are considered as the power sources for the future and the proton exchange membrane fuel cell is one of the most important alternative clean power generators for portable, mobile and stationary applications. PEM fuel cell has low to zero emission, low temperature, high power density and fast start up [1-8]. They use hydrogen as the fuel and are the most popular type of fuel cells. To achieve better operation and performance, better design and optimization is necessary [2]. The flow field design in the bipolar

*Corresponding author: E-mail address: mkermani@aut.ac.ir
Tell/ +98 (21) 6454342

plates is one of the key parameters for the better utilization of catalyst layer (CL) and enhancing the performance of this type of fuel cells. The PEMFC's channels act as reactant distributor. The reactants, as well as the products, are transported to and from the cell through the flow channels. An appropriate flow field design can enhance the reactant transport and the water removal from the cell to minimize the concentration dissipation [1, 3].

Because of slow reaction rates in the cathode side of PEMFCs, this side can be considered as a performance limiting component, so researchers have mainly focused their efforts on the cathode side [9].

In 1998 a novel concept for convective heat transfer enhancement was presented by Guo et al [10].Generally there are three ways to enhance the heat transfer. (1) Increasing the flow velocity, (2) Increasing the wall temperature gradient and (3) Increasing the included angle between the velocity vector and temperature gradient [10].

The concept of enhancing convective heat and mass transfer by reducing the intersection angle between velocity and temperature gradient is called field synergy principle [11-13]. To raise the intersection angle using some partial blocks (indents) along the fluid delivery channel is recommended [6]. In a similar geometry, because of the analogy between heat and mass transfer, the mass exchange between the channel and the catalyst layer in the cathode of the PEMFC is expected to increase in the same order as that in heat transfer, so the oxygen consumption will be enhanced and the performance of the fuel cell will be increased [6]. Choghadi and Kermani [3] show 15% efficiency enhancement in a PEM fuel cell using partially interdigitated serpentine flow field in an experimental test. Perng et al [8] showed that the transverse installation of a rectangular cylinder in the flow channel effectively enhances the cell performance of a PEMFC. Heidary et al. [14] studied the heat transfer and flow field in a wavy channel linked to a porous gas diffusion layer (GDL). They showed that heat transfer in channels can be enhanced up to 100%, depending on the wave amplitude, wave number and flow Reynolds number.

In this paper a commercial computational fluid dynamics (CFD) software package is used to correlate the content of concentration of reacting species in catalyst layer to the dent shapes within the flow delivery channel. The subject of pressure drop along the channels is still under the way and will be discussed in another paper separately.

2. Problem definition

The computational domain consists of a single channel of length 80 mm, connected at the top to a Gas Diffusion Layer (GDL) over which the Catalyst Layer (CL) is placed. Fig. 1(a) shows the schematics of the domain in the case of no dent along the channel. This is called the base case geometry in the present study. To enhance the performance of the cell, some dents are placed along the channel as shown in Figs. 1(b) to 1(d). Various types of dent shapes are used to study the fuel cell performance enhancement. The oxygen reduction reaction occurs within the CL, where CL is assumed to be a porous region, within which oxygen is consumed at a rate of S_{O_2} (with the units of (kg/s)/m^3), and water is formed at the rate of S_{H_2O} ((kg/s)/m^3). These terms are defined in Section 2.3.

2.1. Model assumptions

• Due to the importance of the cathode as the performance limiting component in PEM Fuel Cells, only the cathode side is considered here.
• The flow operates under steady state conditions.
• The working fluid is a gas mixture consisting of the species oxygen, nitrogen and water, which are considered as ideal gas.
• The flow is considered to be laminar.
• The gas diffusion layer, catalyst layer are treated as isotropic porous media.
• Each dent has 10 mm distance from other dents.

2.2. Model geometry

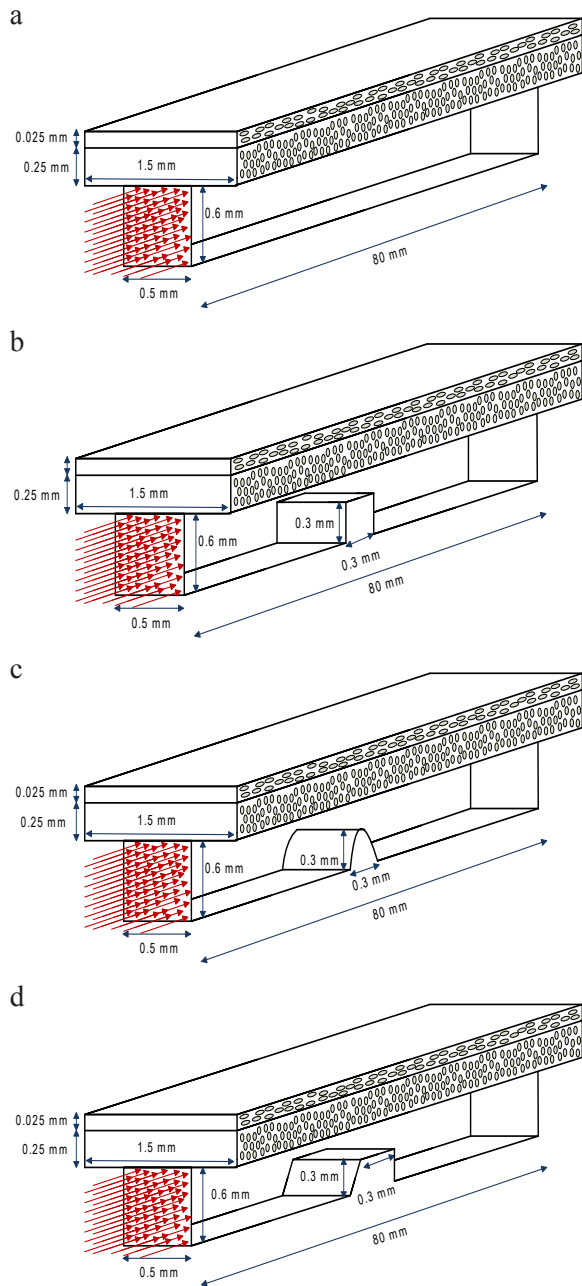Model geometry consists of a gas flow channel, a

Fig. 1.(a). Schematic of the base case geometry containing no dent along the channel, (b). Schematic of a dented channel with square dent profile shape, (c). Schematic of a dented channel with semicircle dent profile shape, and (d). Schematic of a dented channel with trapezoid dent profile shape. It is noted that in real case, six dents are placed along the channel. But for clarity of the dent shapes, only one dent is shown here.

gas diffusion layer and a catalyst layer. Four types of channel configurations are considered: the base case with no dent along the channel, and three cases

with various dent profile shapes of square, semicircle and trapezoid, as shown in Figs 1 and 2. Six equally spaced dents are considered along the channel for the dented cases.
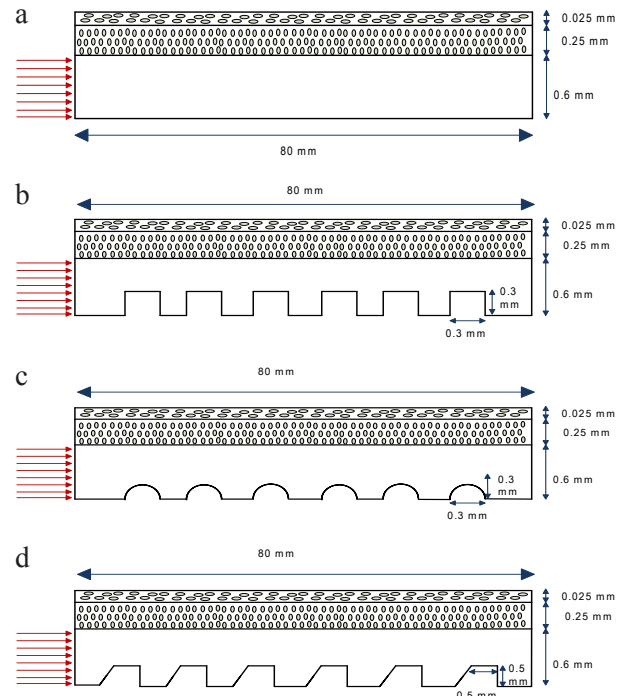

Fig. 2.(a). Schematic of the side view of the base case geometry containing no dent along the channel, (b). Schematic of the side view of the dented channel with square dent profile shape containing six dents along the 80 mm channel, (c). Schematic of the side view of the dented channel with semicircle dent profile shape containing six dents along the 80 mm channel, (d). Schematic of the side view of the dented channel with trapezoid dent profile shape containing six dents along the 80 mm channel.

2.3. Governing equations

The governing equations for the channel (as a clear region) and the GDL and CL are written in a unified form as follows, where the equations contain porosity (ε) and permeability values (k). In channel region ε is set to 1, and $k \rightarrow \infty$ and in GDL and CL regions, the specified values in Table 1 are used for ε and k.

The conservation of mass for the three-species gas mixture is:

$$\frac{\partial(\varepsilon\rho)}{\partial t}+\nabla.\left(\varepsilon\rho\vec{u}\right)= S_{m}, \tag{1}$$

where S_m is the source term of the mixture defined later in this section. The mixture momentum equation within the channel region is:

$$\frac{\partial(\rho\vec{u})}{\partial t}+\nabla.(\rho\vec{u}\vec{u})=-\nabla P+\nabla.(\mu\nabla\vec{u}) \qquad (2)$$

The momentum equation in porous zones of GDL and CL is defined using the Darcy's law as:

$$\varepsilon\vec{u}=\frac{-\kappa}{\mu}\nabla P \qquad (3)$$

The mixture energy equation is:

$$\frac{\partial(\varepsilon.\rho.C_PT)}{\partial T}+\nabla.(\varepsilon.\rho.C_P\vec{u}T)=\nabla.(K^{eff}\nabla T) \qquad (4)$$

The species transport equations are written using the Fick's law as:

$$\frac{\partial(\varepsilon.C_\kappa)}{\partial t}+\nabla.(\varepsilon\vec{u}C_\kappa)=\nabla.(D_\kappa^{eff}\nabla C_\kappa)+S_\kappa \qquad (5)$$

Here S_k is the species source term, where the subscript k represents O_2, H_2O. Within the channel and GDL $S_K=0$, while S_k within the CL is obtained from:

$$S_{O_2}=\frac{-M_{O_2}i}{4F}\frac{A_g}{(Vol.)CL}\left[(kg/s)/m^3\right] \qquad (6)$$

$$S_{H_2O}=\frac{-M_{H_2O}i}{2F}\frac{A_g}{(Vol.)CL_g}\left[(kg/s)/m^3\right] \qquad (7)$$

$$S_m=S_{H_2O}+S_{O_2} \qquad (8)$$

M:　　　　molecular mass
F:　　　　Faraday constant
i:　　　　current density
A_{CL}:　　　CL area, (w+d)L,
$(Vol.)_{CL}$:　the CL volume

To numerically solve the governing equations (Eqns.1-5), a commercial CFD software package is used. Figure 3 and 4 show sample of the grid configurations used in the present study.
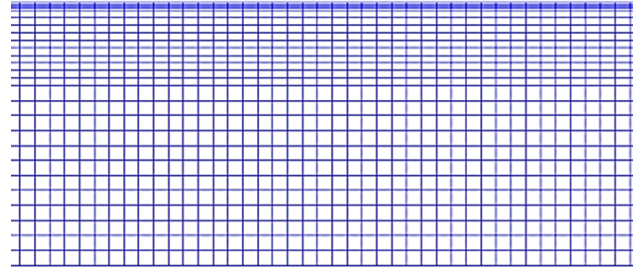

Fig. 3. Sample of the grid configuration for the base case geometry (see Figs. 1(a) and 2(a))
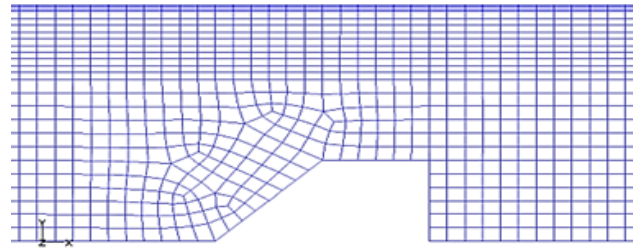

Fig. 4. Sample of the grid configuration for trapezoid dent profile shape (see Figs 1(d) and 2(d))

3. Results and discussion

Computations of a straight channel flow field of a PEM fuel cell is studied in this paper. To enhance the performance of the cell, channel indentations are used in this study. Four cases are considered, including three dented cases, and one undented case referred as the base case in this study. The cell operating conditions are 0.5, 1 and 2 A/cm^2 (three current densities) at 333 K, 1 bar, water dew point temperature 313 K, and 50% oxygen utilization. Complete details are provided in Table 1. The nomenclatures of the computed cases are listed in Tables 2 and 3.

Figures 5 to 7 show contours of oxygen mole fraction at GDL/CL interface for undented case (labeled as ND in Table 2) and dented cases (labeled as SQ, SC and TR in Table 2).

According to Figures 5 to 7, channel indentation increases the content of oxygen at the face of CL. This is due to the synergy effect between diffusion and convection mechanisms that transport oxygen from channel to the CL, hence the performance of the cell increases by channel indentation.

Table 1. Physical properties and geometry.

Current density	2 & 1 & 0.5 A/cm^2
Operating temperature	333K
Operating pressure	101325 Pa
Faraday constant	96487 C Mol^{-1}
Gas constant	8.314 JMol^{-1}K^{-1}
Dew point temperature	313 K
Utilization	50%
Porosity of gas diffusion layer, ε_{GDL}	0.55
Viscous resistance of gas diffusion layer	10-12 m^{-2}
Porosity of catalyst layer, εCL	0.475
Viscous resistance of catalyst layer	10-12 m^{-2}
Channel length	80 mm
Channel height	0.6 mm
Channel width	0.5 mm
GDL height	0.25 mm
CL height	0.025 mm

Table 2. Nomenclature of computed cases (dent profile shapes).

Case name	Dent profile shape	Number of dents along the channel
ND	No dent	---
SQ	Square	6
SC	Semicircle	6
TR	Trapezoid	6

Table 3. Nomenclature of computed cases (operating current densities).

Case name	Current density value A/cm²
NQ$_I$, SQ$_I$, SC$_I$, TR$_I$	2.0
NQ$_{II}$, SQ$_{II}$, SC$_{II}$, TR$_{II}$	1.0
NQ$_{III}$, SQ$_{III}$, SC$_{III}$, TR$_{III}$	0.5

The level of enhancement differs based on the dent profile shapes, with the rank 1 (i.e. the best enhancement) for the trapezoid dent, rank 2 semicircle shape dent, and rank 3 square shape dent.
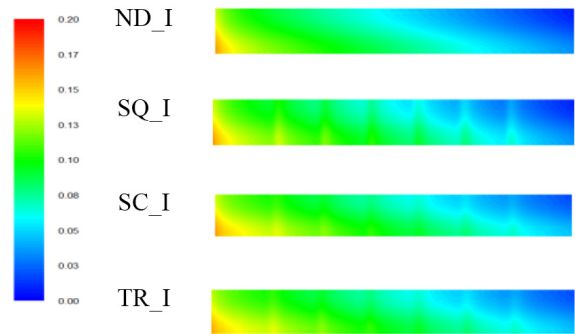

Fig.5. Contour of oxygen mole fraction at GDL/CL interface in i= 2 A/cm².
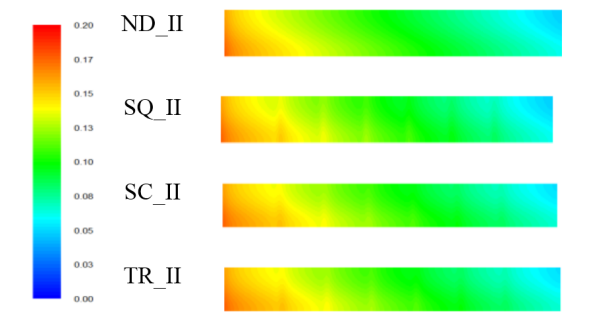

Fig. 6. Contour of oxygen mole fraction at GDL/CL interface in i= 1 A/cm².
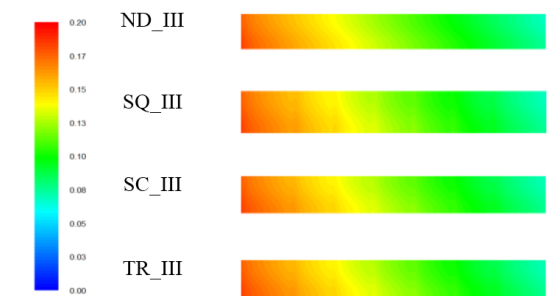

Fig. 7. Contour of oxygen mole fraction at GDL/CL interface in i= 0.5 A/cm²

Figures 8 to 11 represent the variation of oxygen, nitrogen and water vapor mole fraction along the channel.

Figure 8 represents the profile of oxygen, nitrogen and water vapor mole fractions along the channel centerline for the base case (i.e. no dent case). As shown in this figure, due to the oxygen consumption, its mole fraction decreases along the channel. On the other hand, due to formation of water in the cathode electrode, the content of water increases
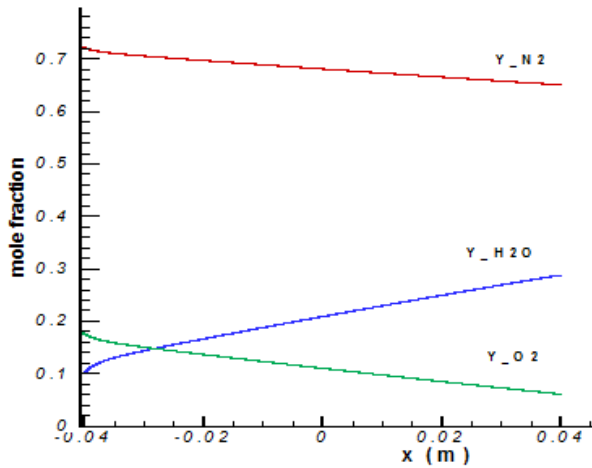
Fig. 8. Sample of the computed results for i=1 A/cm²: profile of oxygen, nitrogen and water vapor mole fractions along the channel centerline for the base case (i.e. no dent case).

simultaneously. The mass (and mole) flow rate of nitrogen remains constant along the channel, but its mole fraction decreases due to the gradual increase of total mass along the channel.

Figures 9 to 11 show the variation of oxygen mole fraction along the channel centerline for various current densities. It is observed that using channel indentation increases the oxygen content along the channel with some peak values right above the dents.
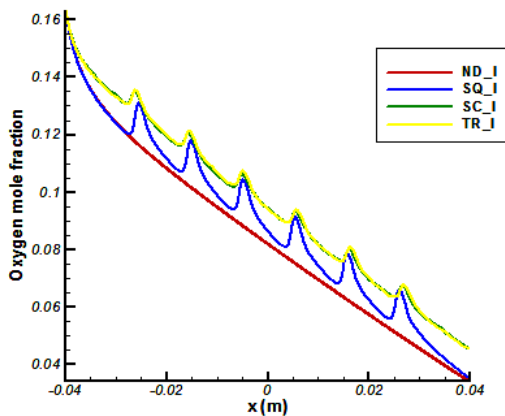

Fig. 9. Sample of the computed results for i=2 A/cm²: comparison of the oxygen mole fraction along the channel centerline for the dented cases with that of the base case. As illustrated here, the best performance is achieved by the trapezoid dent shape.

As a result, the average of oxygen content (e.g. oxygen mole fraction) increases in all areas above the dents including the GDL/CL interface. Then the driving moment for the kinetic of reaction enhances.
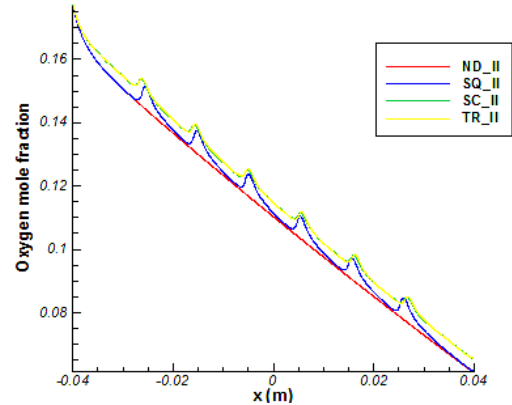

Fig. 10. Sample of the computed results for i=1 A/cm²: comparison of the oxygen mole fraction along the channel centerline for the dented cases with that of the base case. As illustrated here, the best performance is achieved by the trapezoid dent shape.

Fig. 11. Sample of the computed results for i=0.5 A/cm²: comparison of the oxygen mole fraction along the channel centerline for the dented cases with that of the base case. As illustrated here, the best performance is achieved by the trapezoid dent shape.
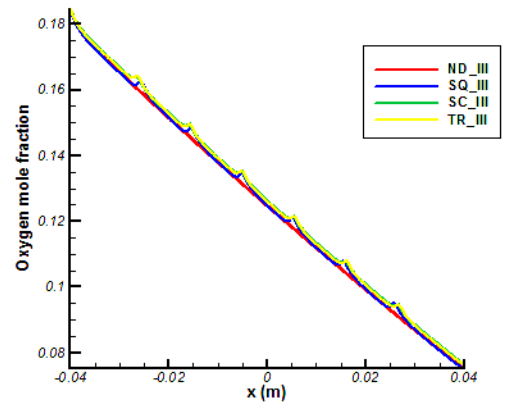
Figures 12 and 13 show the pressure drops along the channel centerline for the dented and undented cases at i=1.0 A/cm². According to Figure12, channel indentation causes excessive pressure drop along the channel. As illustrated in this figure, the case with trapezoid dent profile produces the highest pressure drop along the channel, even higher than that of the

square dent case. In the first glance, this seems to be a bit odd, as the trapezoid dent has more aerodynamic shape than that of the square dent. This is explained as follows.
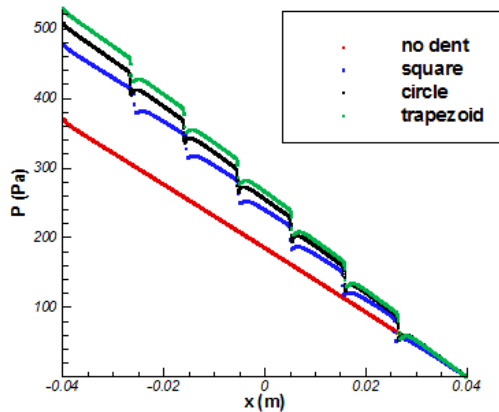

Fig. 12. Pressure drop in channel centerline, i= 1 A/cm².

The trapezoid dents possess the largest wetted area, giving the biggest skin friction, amongst the cases considered in this study, e.g. as compared with the square dent cases. To double check on this matter, a dent with rectangle profile shape and identical wetted area as that of trapezoid is considered, and the pressure drop for these cases are shown in Figure 13 for comparison purposes. As shown in this figure the trapezoid dents produce lower pressure when compared with the rectangle dent cases containing identical wetted surface area.
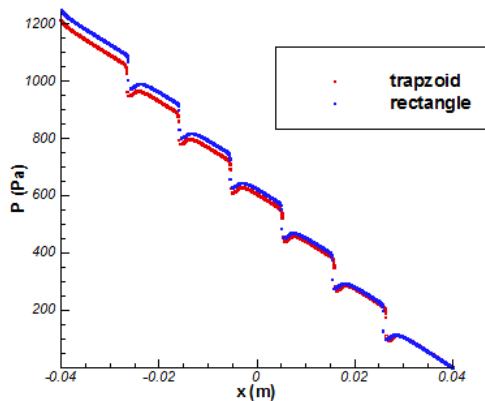

Fig. 13. Pressure drop in channel centerline, i= 2 A/cm², comparison between trapezoid and rectangle dent profile shapes.

Figure 14 shows the relative humidity (ϕ) of flow at GDL/CL interface for i= 1 A/cm². From this figure it can be seen that some regions with ϕ >100% exist within the computation domain. Although ϕ >100% is unrealistic, but in fact this figure provide very valuable pieces of information for the possible locus
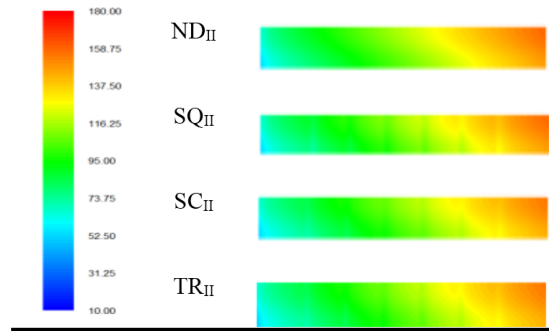

Fig. 14. Relative humidity contour at GDL/CL interface surface, i= 1 A/cm².

of two-phase regions. As illustrated in Figure 14, a considerable portion of the computational domain (about 1/3) is predicted to be two-phase by the present single-phase solver. This large content of condensate should be directed toward the outlet of the channel. This task is performed by a large enough pressure gradient along the channel. Pressure gradient along the channel for all of the cases considered are presented next.

Table 4 summarizes highlights of the results in the present study. The first column of the table shows the geometrical condition of the dents along the channel (previously introduced in Table 2). The second column in Table 4 represents the enhancement ratio of the oxygen content at the face of CL with respect to the base case (i.e. undented case). It is noted that Y_{O_2} in Table 4 represents the area averaged oxygen mole fraction in GDL/CL interface. The last column in Table 4 represents the pressure gradient along the channel for each case.

As shown in Table 4, the value of pressure gradient along the channel varies from 22 to 151mbar/m. These values are sufficient to remove any liquid water from the gas flow channel to avoid flooding in GDL and channel regions.

Table 4. Summary of the results.

Case name	$YO_2/(YO_2)_{B\ Case}$	∇P (mbar/m)
ND_I	1	94.29
SQ_I	1.082	138.29
SC_I	1.176	143.01
TR_I	1.180	151.25
ND_{II}	1	46.25
SQ_{II}	1.018	59.80
SC_{II}	1.046	63.52
TR_{II}	1.047	66.08
ND_{III}	1	22.95
SQ_{III}	1.005	27.80
SC_{III}	1.0142	29.52
TR_{III}	1.0145	30.44

4. Concluding remarks and future works

In this paper it is shown that channel indentation can increase the content of oxygen in CL up to 18%. This is driving moments for the kinetics of reaction within the CL. In this paper solely the mechanisms of increasing oxygen consumption as a driving moment are discussed. It is noted that channel indentation in one hand increases the kinetics of reaction and in turn the electrical power produced by the cell. But, on the other it causes excessive pressure drop along the channel and extra pumping power is required. This introduces an interesting optimization subjects considering the influences on the net power that is planned for near future.

Acknowledgement

5. References

[1] Wang X., Duan Y., Yan W. and Peng X., "Local transport phenomena and cell performance of PEM fuel cells with various serpentine flow field designs", J. Power Sources, 2008, 175:397.

[2] Ramesh P. and Duttagupta S.P., "Effect of channel dimensions on Micro PEM fuel cell performance using 3D modeling", Int. J. Renewable Energy Research, 2013, 3, No. 2.

[3] Choghadi H.R. and Kermani M.J., "15% efficiency enhancement using novel partially interdigitated serpentine flow field for PEM fuel cells", 10Th International Conference on Sustainable Energy Technologies SET2011, Istanbul, Turkey, 4-7 Sep. 2011.

[4] Bernardi D.M. and Verbrugge M.W., "A mathematical model of the solid-polymer-electrolyte fuel cell", J. Electrochem.1992, 139.

[5] Khakbaz Baboli M. and Kermani M.J., "A two-dimensional, transient, compressible isothermal and two-phase model for the air side electrode of PEM fuel cell", J. Electrochemical Acta, 2008, 53:7644

[6] Heidary H. and Kermani M.J., "Performance enhancement of fuel cells using bipolar plate duct indentations', Int. J. Hydrogen Energy, 2012, 38:5485.

[7] Yuan W., Tang Y., Pan M., Z. Li and Tang B., "Model of prediction of effects of operating parameters on proton exchange membrane fuel cell performance", J. Renewable Energy, 2010, 35:656.

[8] Perng S.W., Wu H.W., Jue T.C. and Cheng K.C., "Numerical predictions of a PEM fuel cell performance enhancement by a rectangular cylinder installed transversely in the flow channel", J. Applied Energy, 2009, 86:1541.

[9] Natarajan D. and Van Nguyen T., "A two dimensional two phase multi component transient model for the cathode of a proton exchange membrane fuel cell using conventional gas distributors", J. Electrochemical Society, 2001, 148:1324.

[10] Guo Z.Y., Li D.Y. and Wang B.X., "A novel concept

for convective heat transfer enhancement", Int. J. Heat and Mass Transfer, 1998, 41:2221.

[11] Tao W.Q., Guo Z.Y. and Wang B.X., "Field synergy principle for enhancing convective heat transfer its extension and numerical verifications", Int. J. Heat and Mass Transfer, 2002, 45:3849.

[12] Tao W.Q., He Y.L., Wang Q.W., Qu Z.G. and Song F.Q., "A unified analysis on enhancing single phase convective heat transfer with field synergy principle", Int. J. Heat and Mass Transfer, 2002, 45:4871.

[13] Guo Z.Y., Tao W.Q. and Shah R.K., "The field synergy (coordination) principle and its applications in enhancing single phase convective heat transfer", Int. J. Heat and Mass Transfer, 2005, 48:1797.

[14] Heidary H. and Kermani M.J., "Enhancement of heat exchange in a wavy channel linked to a porous domain; a possible duct geometry for fuel cells", Int. J. Heat and Mass Transfer, 2012, 39:112.